Memoirs of the College of Science, University of Kyoto, Series A,
Vol. XXX, No. 2, Article 1, 1962.

OBSERVATIONAL RESULTS OF THE THREE-COLOR PHOTOMETRY WITH A DISCUSSION ON THE RELATIVE LOCATIONS OF GIANTS AND SUPERGIANTS TO THE MAIN SEQUENCE IN THE COLOR DIAGRAM

BY

Tsutomu SHIMIZU, Fumihiko IMAGAWA
and Kazutomo TAKAYANAGI

(*Received November, 16, 1961*)

ABSTRACT

The results of the three-color photoelectric observations of standard stars are reported, with a brief description of our apparatus. The observed colors for these stars are listed in Table 1. The two-color diagram obtained is illustrated in Fig. 5. It is noticed there that (i) clear separation of the luminosity class III from the class V is seen and (ii) the class I looks as if it were also distinguishable from the other two, but it may be due to the space reddening. Concerning the locations of the giants and supergiants relative to the main sequence on the diagram estimated quantitatively by use of Stebbins-Whitford's six-color photometric data, those of the formers coincide well with our observational data as they stand, while those of the latters deviate in respective amounts just as nearly expected from the reddening corrections based on Arp's preliminary intrinsic colors. The second fact may not only serve as a verification of Arp's intrinsic color but also open a way for evaluating the space reddening of supergiants.

1. Photometric apparatus

From autumn, 1959 the *U, B, V* photoelectric observation with the use of a 30 cm Cooke-refractor was started at our observatory.

The photometric apparatus is of a conventional construction. A general view of the apparatus is shown in the accompanying picture. Fig. 1 shows the photometer head; the principal parts of which are as follows: a field-finding eyepiece, a focal-plane setting eyepiece, focal-plane diaphragms, a filter-holder, a Fabry lens, an RCA 1P21 photomultiplier and an ice-box. Either of the eyepieces is arranged by a diagonal prism so as to be withdrawn from the light beam except when a star image in the diaphragm is looked at for certifying. The focal-plane diaphragms are 0.5, 1, 2 and 10 mm in diameter, corresponding to 20″, 40″, 80″ and 400″ respectively, among which the 2 mm-diaphragm has been mostly used. A set of diaphragms as well as that of filters are inserted in respective rotatable plates

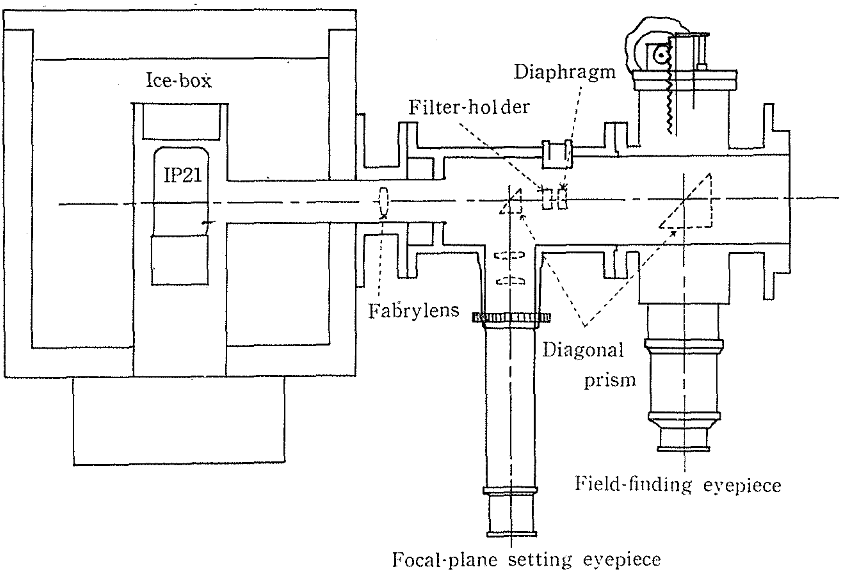

Fig. 1. Schematic diagram of the photometer head.

by which their quick and smooth exchanges are possible, instead of sliding plates. A Fabry lens through which the exit pupil of the telescope objective is imaged on the cathod of the photomultiplier, is used for letting the effect of the guiding error be free so long as the star image is within the diaphragm. The photomultiplier can be refrigerated with dry-ice in the ice-box, though no such operation is necessary for the stars brighter than the 8 th magnitude. The filters used are as follows:

Color	U	B		V
Filter	$UV-D2$	$V-V2+$	$UV-39$*	$V-03C$
Thickness (mm)	1	1	1	2

* For cut-off of the ultraviolet radiation.

These were selected from Matsuda glass filters so that their transmissions might resemble to those of Johnson's standard system (**1**) as closely as possible. The response curve of each filter combined with the photomultiplier 1P21 is shown in Fig. 2. With regard to the transmission of the refractor objective, it will be mentioned in a later section.

The D. C. amplifier designed by us was at first of a type not so much different from Kron's (**2**) and was made at Nippon Denkikizai Co., Ltd. Its circuit diagram with that of the power supply is shown in Figs. 3A and 3B. The

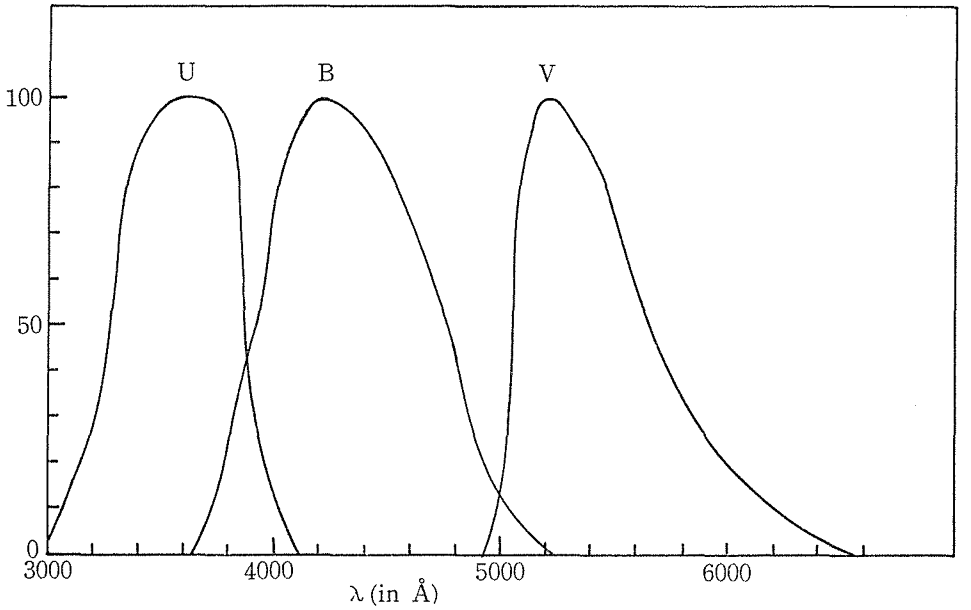

Fig. 2. Response bands of our system, taking no account of refractor objective.

input resistance can be switched in 3 steps of every 2.5 magnitudes by S_1 (coarse sensitivity) ; the negative feedback is variable in 6 steps of every 0.5 magnitudes by S_2 (precision sensitivity : the resistance for the highest sensitivity being 100 Ω).

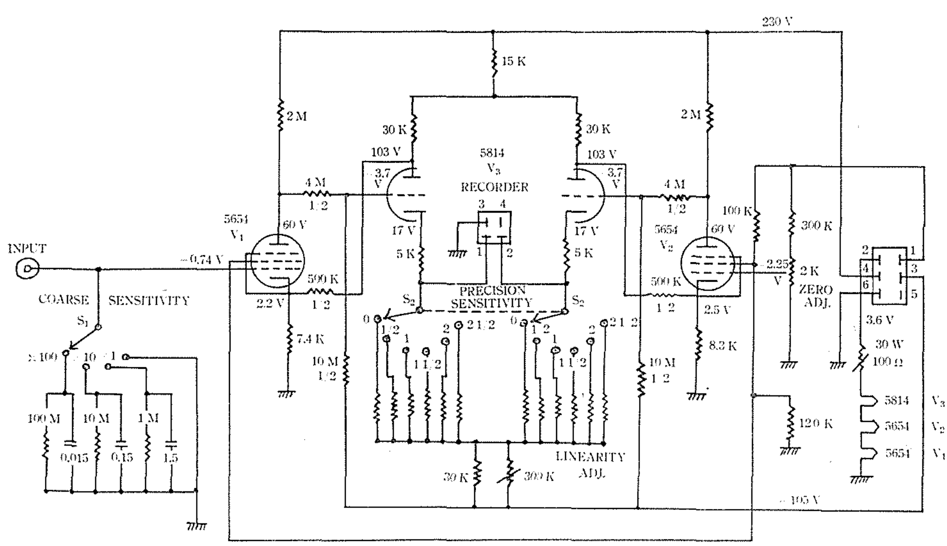

Fig. 3A. Circuit diagram of the amplifier.

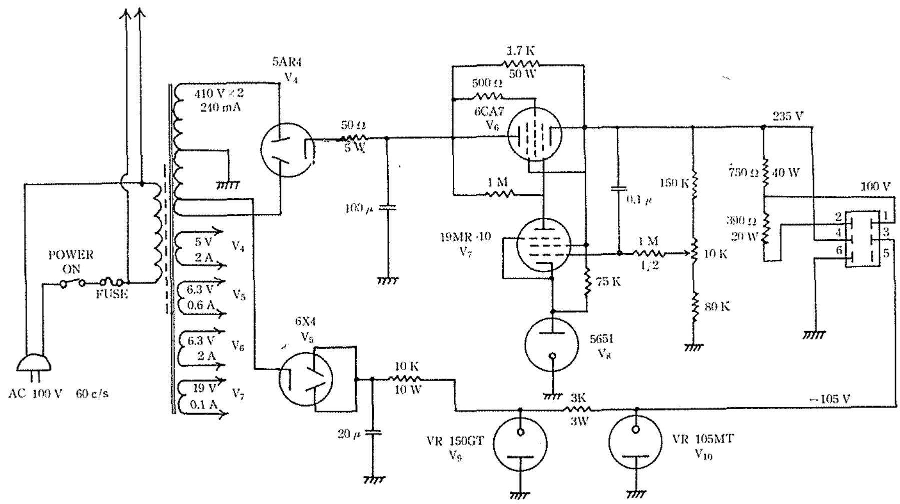

Fig. 3B. Circuit diagram of the power-supply.

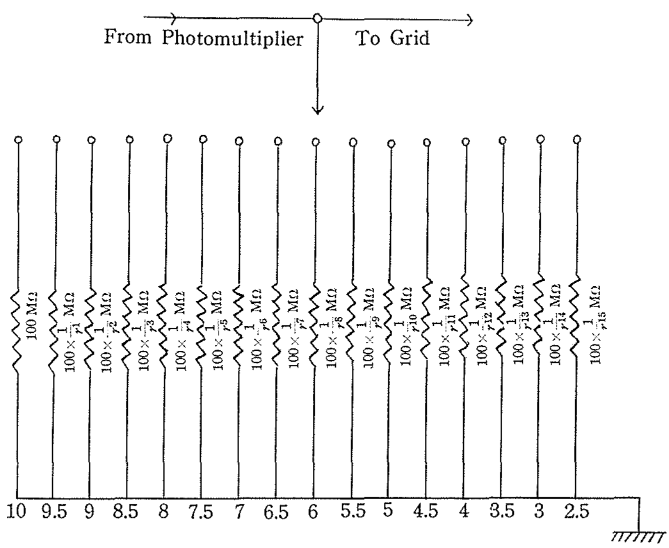

Fig. 3C. Circuit diagram of the attenuator. r represents Pogson's light ratio 1.58489.

After several months since its construction, however, it was found that the linearity of the amplifier was unsatisfactory for switching S_2 on 1, $1\frac{1}{2}$, 2 and $2\frac{1}{2}$. Hence, S_1 was replaced with the newly devised attenuator for letting these steps in S_2 be out of use. This attenuator has 15 steps of every 0.5 magnitude interval as indicated in the circuit diagram in Fig. 3 C. The test measurements of the linearity of the amplifier illustrated in Fig. 4 showed that deviations from the linearity do not exceed 1% over the whole measurable range, or from 0 up to 10 mV of the output voltage. The zero-point drift of the amplifier is also kept within 1% after a warm-up period of 30–40 minutes. The high voltage of the 1P21 is supplied by the integrating dry batteries, keeping 900 V for all the stars less luminous than the 2 nd magnitude. In order to avoid the effect of the interbattery leakage which is so serious in such a place of high humidity as in Kyoto, each battery was enveloped with thin membrane of paraffin. This has been proved very effective.

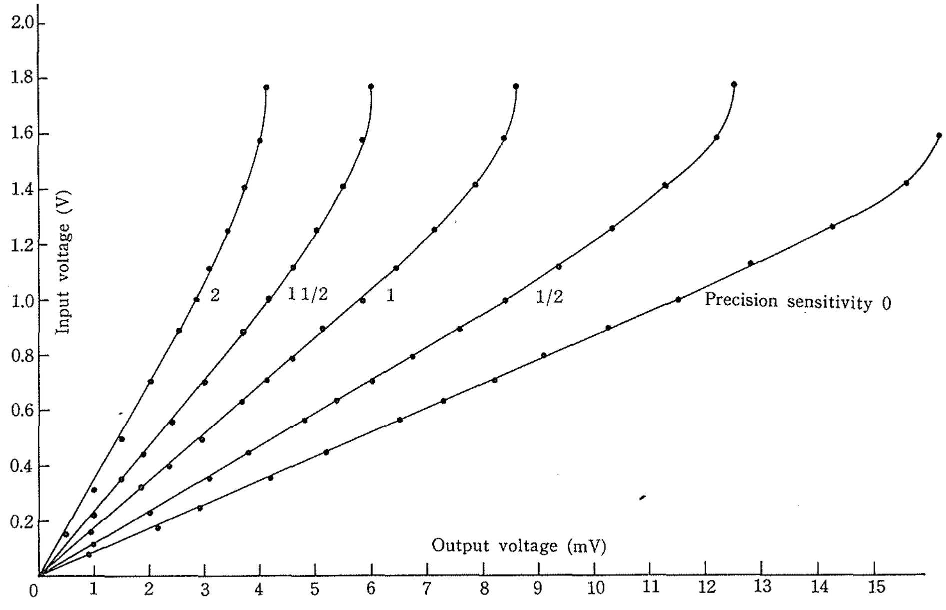

Fig. 4. Linearity of the amplifier. Input voltage is in arbitrary scale.

Recordings of the measurements are taken with the aid of a 10 mV Brown recording potentiometer with the time-constant of 3 seconds manufactured by Yokogawa Electric Works Co., Ltd. According to the manufacturer the accuracy of recording is to be within 0.5%. Full scale deflection on the recorder corresponds to a maximum current sensitivity of 0.7×10^{-11} amperes. To get rid of long period variation of A. C. input, the voltage stabilizer with the saturable reactor as its regulation element is utilized, in the stage prior to the power supply of the D. C. amplifier.

2. Observations and reductions

We have observed about 70 standard stars taken from the lists of Johnson-Harris (3), Johnson-Morgan (4) and Johnson (5). These stars were selected so as to be distributed evenly in the right ascension and yet to include various kinds of stars respecting the spectral type as well as the luminosity class.

Our observations were carried out mainly in the east side of the meridian in order to lessen the influence of the scattered light from Kyoto City. And even when it was obliged to observe in the west side, the observed zenith distances were restricted within 30° and yet these results were separately reduced from those in the east side at the same night.

A single observation consisted of the deflection recordings of the three colors (V, B, U in succession) of the star and the sky, and then the dark if required. No return recordings were made because it seemed preferable to gain more independent observations.

The observed color indices $C_{(B-V)_0}$ and $C_{(U-B)_0}$ obtained from the deflections were reduced to the ones outside the atmosphere C_{B-V} and C_{U-B} in the usual way, either by the method of least squares or the graphical means. Namely,

$$\left.\begin{aligned} C_{B-V} &= C_{(B-V)_0} - K_{B-V} \sec Z\,, \\ C_{U-B} &= C_{(U-B)_0} - K_{U-B} \sec Z\,, \end{aligned}\right\} \qquad (1)$$

where

$$\left.\begin{aligned} K_{B-V} &= k_1 + k_2 C_{B-V}\,, \\ K_{U-B} &= k_3 + k_4 C_{U-B}\,. \end{aligned}\right\} \qquad (2)$$

But, when such a linearity between K and C as assumed in (2) could hardly be settled among all the stars obsrved in a given night owing to the fluctuated deviations from the uniform atmosphere or to the low intensity of U color, the mean K for all the stars in that night was adopted by taking no account of (2). The sky conditions at Kyoto are quite different from season to season, night to night and yet liable to change from time to time, so that though we selected only the nights thought as in a fairly good condition, it resulted that the extinction coefficients were in a range of 0.11–0.30 mag. for K_{B-V} and 0.25–0.59 mag. for K_{U-B}.

For a single night observation, the probable errors of our color indices were found to be

C_{B-V}: 0.01–0.05 mag.; mean of p. e. = 0.02 mag.
C_{U-B}: 0.02–0.12 mag.; mean of p. e. = 0.05 mag.

Low accuracy in C_{U-B} is due to strong ultraviolet absorption in the refractor objective as will be mentioned later.

Our color indices C_{B-V} and C_{U-B} were compared with those of Johnson's standard system. Between C_{B-V} and $B-V$, the correlation was found to be well represented with a linear expression as follows:

$$B-V = (0.991 \pm 0.010) C_{B-V} + 0.751 \pm 0.006 . \qquad (3)$$

While, between C_{U-B} and $U-B$, such a linear one could hardly hold without appreciable loss of accuracy. This is rather natural because our system is based on the refractor whereas Johnson's is on the aluminized reflector. Then, the blue color index will be discussed in terms of $B-V$ transformed with (3) but the ultraviolet one will be refered to our C_{U-B} as it stands.

3. Results and discussions

The results of our three-color photoelectric observations are listed in Table 1. The two-color diagram for all the stars therein is shown in Fig. 5 where crosses, crosses enclosed by circles, open circles and filled circles denote the stars of the

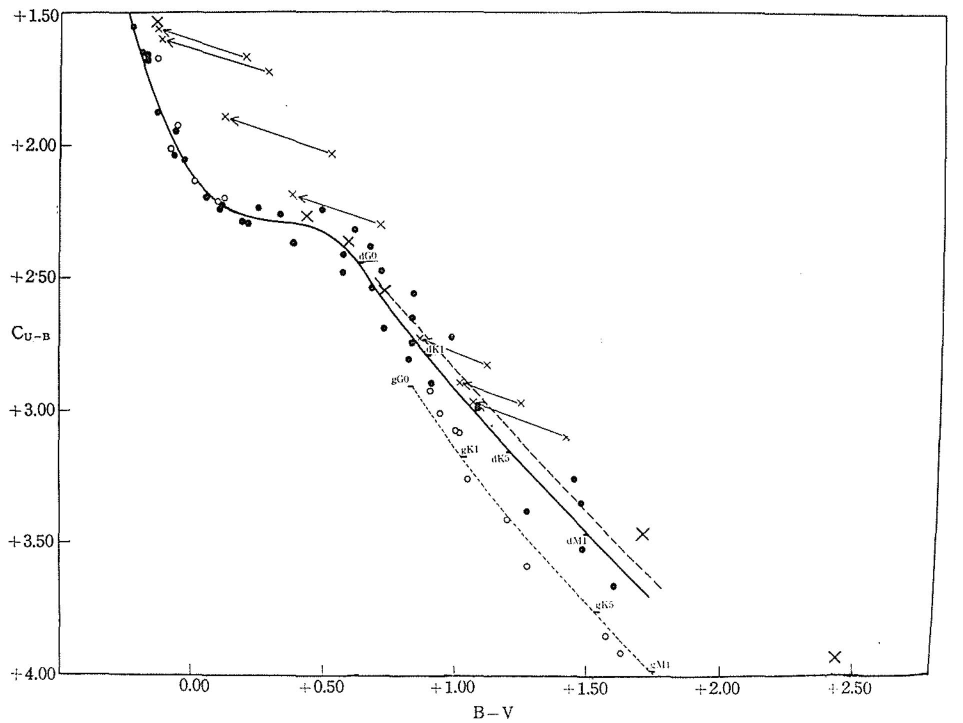

Fig. 5. Two-color diagram of the observed stars. Filled circles are the luminosity class V; open circles are III or IV; crosses are I and crosses enclosed by circles are II. The solid line represents the mean curve for the main sequence stars. The dotted and dashed lines are explained later in the text.

Table 1. Results of the photometric observations. Stars are selected from Johnson-Harris and Johnson-Morgan's standard stars. The 6th column gives the number of observations and the 7th and 8th columns give our photometric data, while the last column gives the value given by Johnson-Harris or Johnson-Morgan. The other columns are self-explanatory.

Ser. No.	HD	Name	α (1950.0)		δ	n	$B-V$	C_{U-B}	$Sp.$	V
			h	m						
1	1013	χ Peg	0	12.0	+19° 56′	3	+1.62	+3.89	M2 III	4.80
2	1280	θ And	0	14.5	+38 24	4	+0.05	+2.18	A2 V	4.61
3	2905	κ Cas	0	30.1	+62 39	4	+0.20	+1.64	B1 Ia	4.15
4	3651	54 Psc	0	36.8	+20 59	3	+0.82	+2.63	KO V	5.84
5	4614	η Cas	0	46.1	+57 33	4	+0.60	+2.30	GO V	3.45
6	4727	ν And	0	47.0	+40 48	4	−0.13	+1.88	B5 V	4.53
7	6582	μ Cas	1	04.9	+54 41	4	+0.71	+2.45	G5 Vp	5.12
8	6961	θ Cas	1	08.0	+54 53	1	+0.24	+2.22	A7 V	4.33
9	7927	ϕ Cas	1	16.9	+57 58	4	+0.70	+2.28	FO Ia	4.95
10	9927	51 And	1	34.9	+48 23	4	+1.27	+3.57	K3 III	3.56
11	10476	107 Psc	1	39.8	+20 02	4	+0.82	+2.71	K1 V	5.23
12	10780	HR 511	1	44.1	+63 36	4	+0.80	+2.79	dK2	5.63
13	12929	α Ari	2	04.3	+23 14	2	+1.19	+3.39	K2 III	1.99
14	13974	δ Tri	2	14.0	+34 00	4	+0.66	+2.36	GO V	4.87
15	15318	ξ^2 Cet	2	25.5	+ 8 14	1	−0.09	+2.00	B9 III	4.28
16	16160	HR 753A	2	33.3	+ 6 39	2	+1.07	+2.97	dK4	5.82
17	19373	ι Per	3	05.5	+49 25	3	+0.67	+2.52	GO V	4.04
18	20630	κ Cet	3	16.7	+ 3 11	3	+0.68	+2.70	G5 V	4.82
19	20902	α Per	3	20.7	+49 41	3	+0.56	+2.35	F5 Ib	1.80
20	21120	o Tau	3	22.1	+ 8 51	4	+0.89	+2.90	G8 III	3.59
21	21291	HR 1035	3	25.0	+59 46	3	+0.52	+2.01	B9 Ia	4.23
22	22049	ε Eri	3	30.6	− 9 38	3	+0.89	+2.87	K2 V	3.73
23	24398	ζ Per	3	51.0	+31 44	3	+0.29	+1.69	B1 Ib	2.83
24	27371	γ Tau	4	16.9	+15 31	2	+0.99	+3.05	KO III	3.65
25	27697	δ Tau	4	20.0	+17 26	2	+1.00	+3.06	KO III	3.76
26	28305	ε Tau	4	25.7	+19 04	5	+1.03	+3.24	KO III	3.54
27	30652	π^3 Ori	4	47.1	+ 6 53	6	+0.48	+2.22	F8 V	3.19
28	30836	π^4 Ori	4	48.5	+ 5 31	6	−0.13	+1.66	B2 III	3.69
29	32630	η Aur	5	03.0	+41 10	1	−0.18	+1.65	B3 V	3.17
30	33111	β Eri	5	05.4	− 5 09	1	+0.11	+2.18	A3 III	2.80
31	36512	υ Ori	5	29.5	− 7 20	3	−0.23	+1.54	BO V	4.63
32	38678	ζ Lep	5	44.7	−14 50	5	+0.09	+2.20	A2	3.55
33	38899	134 Tau	5	46.7	+12 38	5	−0.06	+1.91	B9 IV	4.90
34	56537	λ Gem	7	15.2	+16 38	5	+0.10	+2.22	A3 V	3.58
35	58946	ρ Gem	7	25.9	+31 53	5	+0.33	+2.25	FO V	4.16

Table 1. (Continued)

Ser. No.	HD	Name	α (1950.0)	δ	n	$B-V$	C_{U-B}	*Sp.*	*V*
			h m						
36	62345	κ Gem	7 41.4	+24° 31′	5	+0.93	+2.99	G8 III	3.57
37	69267	β Cnc	8 13.8	+ 9 20	4	+1.46	+4.23	K4 III	3.52
38	74280	η Hya	8 40.6	+ 3 35	4	−0.18	+1.66	B3 V	4.30
39	79469	θ Hya	9 11.8	+ 2 32	4	−0.06	+1.93	AOp	3.88
40	87696	21 LMi	10 04.5	+35 29	2	+0.18	+2.27	A7 V	4.48
41	88230	Gmb 1618	10 08.1	+49 42	2	+1.47	+3.33	dMO	6.59
42	89021	λ UMa	10 14.1	+43 10	2	+0.01	+2.11	A2 IV	3.45
43	91316	ρ Leo	10 30.2	+ 9 34	2	−0.14	+1.53	B1 Ib	3.85
44	95735	Lal 21185	10 00.1	+36 18	2	+1.59	+3.64	M2 V	7.47
45	102870	β Vir	11 48.1	+ 2 03	1	+0.56	+2.39	F8 V	3.61
46	106591	δ UMa	12 13.0	+57 19	1	+0.10	+2.21	A3 V	3.31
47	111631	Cin 1633	12 48.1	− 0 29	2	+1.44	+3.24	M0.5 V	8.49
48	113139	78 UMa	12 58.6	+56 38	1	+0.37	+2.38	F2 V	4.93
49	116842	80 UMa	13 23.2	+55 15	1	+0.20	+2.28	A5 V	4.01
50	157881	+2° 3312	17 23.3	+ 2 10	3	+1.43	+3.13	K7 V	7.54
51	159181	β Dra	17 29.3	+52 20	4	+0.97	+2.71	G2 II	2.9
52	163506	89 Her	17 53.4	+26 03	4	+0.43	+2.24	F2 Ia	5.48
53	176437	γ Lyr	18 57.1	+32 37	1	−0.07	+1.96	B9 III	3.25
54	177724	ζ Aql	19 03.1	+13 47	1	−0.04	+2.04	AO	2.99
55	188512	β Aql	19 52.9	+ 6 17	2	+0.84	+2.73	G8 IV	3.71
56	194093	γ Cyg	20 20.4	+40 06	4	+0.71	+2.52	F8 Ib	2.2
57	195593	44 Cyg	20 29.1	+36 46	3	+1.11	+2.81	F5 Iab	6.17
58	196867	α Del	20 37.3	+15 44	2	−0.08	+2.02	B9 V	3.77
59	200905	ξ Cyg	21 03.1	+43 44	3	+1.70	+3.44	K5 Ib	4.1
60	201091	61 CygA	21 04.7	+38 30	3	+1.25	+3.37	K5 V	5.19
61	201092	61 CygB	21 04.7	+38 30	3	+1.47	+3.51	K7 V	6.02
62	206859	9 Peg	21 42.2	+17 07	1	+1.24	+2.95	G5 Ib	4.4
63	206936	μ Cep	21 42.0	+58 33	1	+2.44	+3.91	M2 Ia	3.99
64	214680	10 Lac	22 37.0	+38 47	2	−0.19	+1.64	O9 V	4.88
65	215182	η Peg	22 40.7	+29 58	3	+0.83	+2.54	G2 II–III	2.96
66	217476	HR 8752	22 58.0	+56 41	2	+1.41	+3.08	GO Ia	4.99
67	218329	55 Peg	23 04.5	+ 9 08	3	+1.56	+3.82	M2 III	4.50
68	222368	ι Psc	23 37.4	+ 5 21	2	+0.55	+2.48	F7 V	4.13
69	224930	85 Peg	23 59.6	+26 49	3	+0.69	+2.19	G2 V	5.75

luminosity class of I, II, III–IV and V respectively, and large crosses are the supergiants thought as little reddened and small ones are those clearly reddened. No reddening is needed to take account for the dwarfs and normal giants plotted in the diagram. A solid line is drawn there to represent the mean curve of the main sequence. Scatterings from this line are ascribable mostly to the errors in U magnitude.

In Fig. 5 it is readily seen that the stars belonging to the different luminosity classes of V, III and reddened I are distributed along three different branches whose separations are the more remarkable as the spectral type advances to the later. These branches do not lie in the luminosity order, but the supergiant's

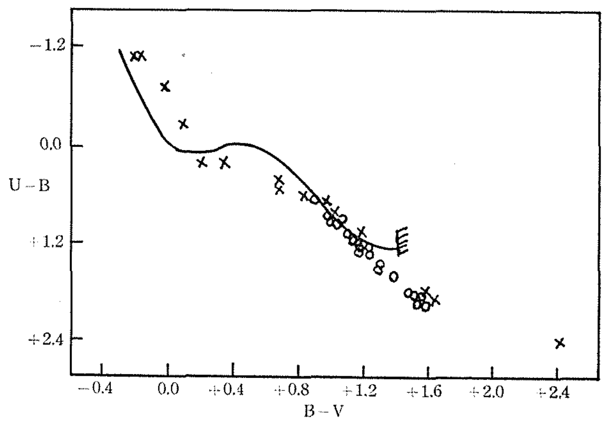

Fig. 6. Two-color diagram of Johnson's standard system. Symbols are the same as in Fig. 5.

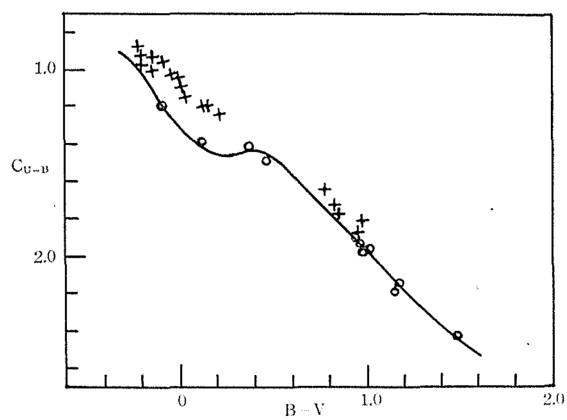

Fig. 7. Two-color diagram of Arp's system. Symbols are the same as in Fig. 5. Plotted stars consist of Johnson-Morgan's and E-Region standards.

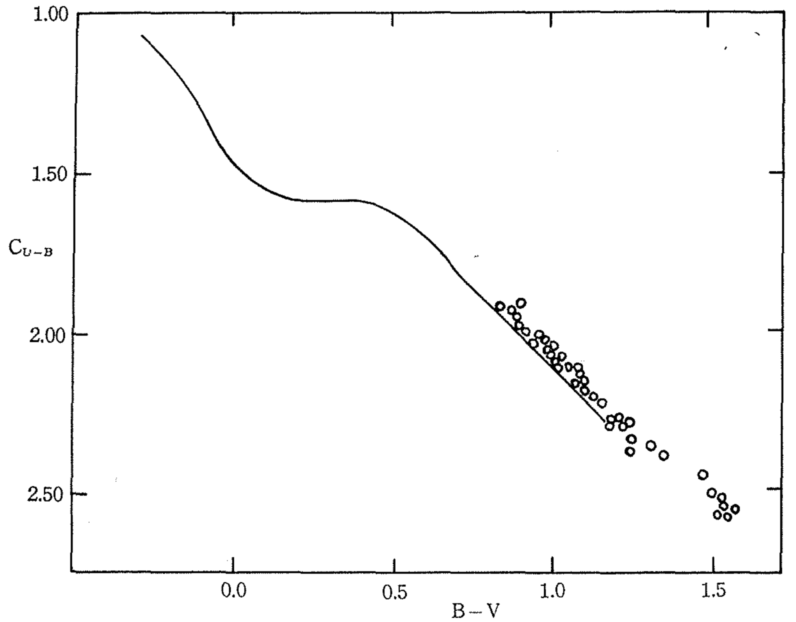

Fig.. 8. Two-color diagram of Cape's system. Symbols are the same as in Fig. 5. Plotted stars consist of E-Region standards.

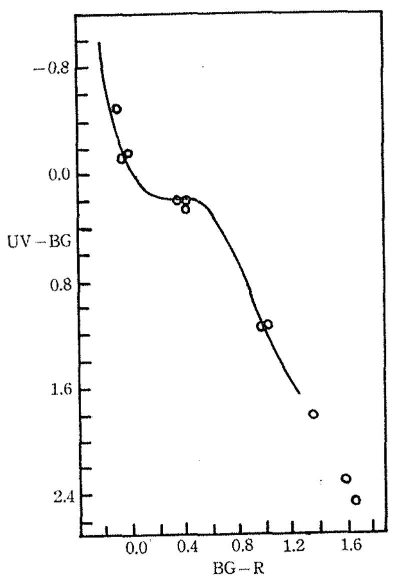

Fig. 9. Two-color diagram of Tifft's system. Symbols are the same as in Fig. 5. Plotted stars consist of the standards in and near NGC 6910 and NGC 6913 and Johnson-Morgan's.

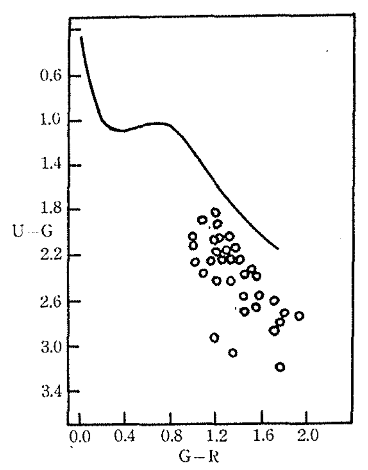

Fig. 10. Two-color diagram of Becker's system. Symbols are the same as in Fig. 5. Plotted stars consist of dwarfs in Pleiades and Praesepe, and giants in six various open clusters.

and the normal giant's locate on the opposite sides of the main sequence branch.

In order to see whether such a feature appears particularily in our two-color diagram or not, let us compare ours with those of Johnson (**4**), Arp (**6**), Cape Observatory (**7**), Tifft (**8**) and Becker (**9**) which are reproduced in Figs. 6~10 from their respective papers. Glancing at these figures, followings may be mentioned.

(i) With respect to the dwarfs there is nothing to say especially. All of the two-color diagrams show samely a depression of the main sequence curve at about A type owing to the well-known effect of absorption in the Balmer limit.

(ii) Concerning the normal yellow giants, however, a variety is pointed out. Separation of the yellow stars between the normal giants and dwarfs can hardly be detected in the diagrams of Johnson (Fig. 6), Arp (Fig. 7) and Tifft (Fig. 9). Whereas it is seen in our diagram (Fig. 5), Cape's (Fig. 8) as well as Becker's (Fig. 10). But, the location of giant's branch is below the main sequence in both of ours and Becker's, while vice versa in Cape's.

(iii) As to the supergiants space reddening must be taken into consideration. Referring to our $B-V$ with the preliminary intrinsic $B-V$ proposed by Arp (**10**), we obtained the color excess in $B-V$, E_{B-V}. On the other hand, we required the ratio of the two-color excesses $E_{C_{U-B}}/E_{B-V}$ by making use of the data of the B1 stars. It becomes

$$E_{C_{U-B}}/E_{B-V} = 0.42\,.$$

Table 2. List of telescopes, photomultipliers and filters used in various systems. Our filters are all of "Matsuda". C designates "Corning" and the others are of "Schott".

Ours	12″ Refr.	RCA 1P 21	U : UV-D2 B : V-V2+UV-39 V : V-03C
Johnson	13″, 82″ Refl.	RCA 1P 21	U : C9863 B : C5030+GG13 V : C3384
Tifft	60″, 100″ Refl.	EMI 6094	UV : C5970 BG : C5030+C3387 R : C2434
Arp	24″ Refr.	EMI	U : C9863 B : BG12+GG13 V : Omag 302 (GG11)
Cape	13″ Astrg. 24″ Refr.	EMI	Ditto
Becker		Photographic plates	U : UG 2 G : GG 5 R : RG 1

By means of such process the reddening corrections for the reddened supergiants can be estimated as represented by arrows in Fig. 5. Supergiants earlier than A with less Balmer absorption appear above the main sequence in all the diagrams including these stars. Even in the diagrams lacking these stars, such situation would be expected if they were added in. Concerning the later types, however, some differences are found among the diagrams. In Johnson's one (Fig. 6) the branch of the supergiant merges into that of the main sequence at about K1, after crossing below the latter at about A 7, while in both Arp's (Fig. 7) and ours (Fig. 5) the supergiant's branch lies always above or on the main sequence.

It seems clear that the differences in the general features on the different two-color diagrams as seen above are ascribable to the different color responses of the whole photometric apparatus including the telescope objectives. In Table 2 is given a list indicating the information about the telescopes, the photomultipliers and the filters used by the different investigators. The relative total response curves are illustrated in Fig. 11 and the corresponding effective wavelengths are tabulated in Table 3. We will compare our response with others'.

(a) Our total response curve is rather different from Johnson's due to the rapid increase of absorption beginning from about 4200 A in our refractor objective, in spite of the similarity of both responses excluding the objectives as shown in Fig. 2. That is to say, the ultraviolet radiation beyond 3500 A is almost

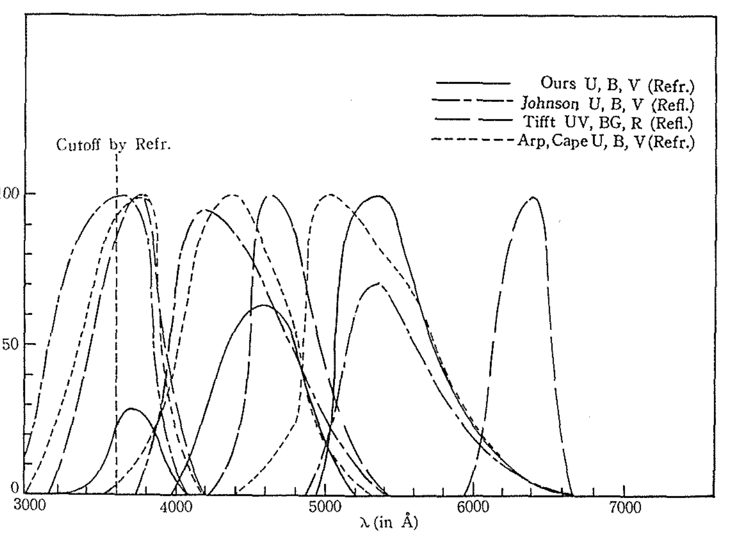

Fig. 11. Comparison of the relative total response, including that of the telescope objective, among various systems.

Table 3. Comparison of the effective wavelength in Å on each system.

	Ours	Johnson	Tifft	Becker
U	3700	3730	3750 (UV)	3730
B	4600	4300	4600 (BG)	4700 (G)
V	5400	5500		
(R)			(6400)	(6380)

cut off by the telescope, so that our *U*-measure is restricted in the narrow band nearly between 3500 A and 3900 A in which the Balmer limit exists. Concerning our *B*, on the other hand, its effective wavelength shifts to the longer side, so ours is nearer to Becker's and Tifft's rather than to Johnson's in this respect. Furthermore, our relative sensitivity of *U*, *B* and *V* are in reverse order with Johnson's.

(b) As regards both Arp's and Cape's responses, we are only informed from their papers (**6**, **7**) that their *U*-measures are limited almost exclusively to the band of 3600-3800 A owing to the use of refractors. On this point our response seems to resemble to theirs, though our *U* sensitivity may be lower than theirs.

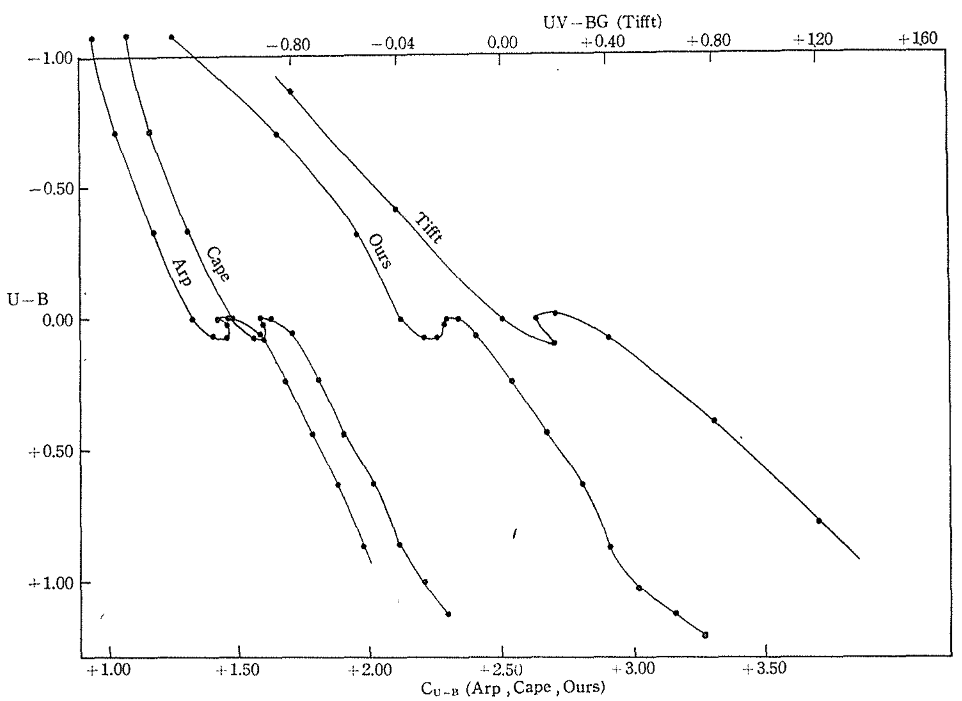

Fig. 12. Comparison of C_{U-B}'s of various systems against the standard $U-B$.

Taking above-mentioned circumstances into consideration, let us compare the ultraviolet color index among Cape's, Arp's, ours and Tifft's in terms of Johnson's $U-B$. First three are based on the refractor while the last or Tifft's is made use of the reflector, nevertheless, cut off the radiation shorter than 3400 A by the filter. With the aid of the tables (**6**, **7**, **8**) published by the respective investigators and Johnson-Morgan's table of intrinsic colors (**4**), each correlation curve between these ultraviolet color indices and Johnson's $U-B$ is required with respect to the main sequence as in Fig. 12. As for ours, it is based on Table 4 read from the mean curves in Fig. 5. From Fig. 12 it is clearly seen that a remarkable duplicate turning at about $U-B=0.0$ appears commonly in any of the four curves. Let us call such photometric systems those of refractor type.

Table 4. Adopted relation between $B-V$ and C_{U-B} read from the mean curves in our two-color diagram.

$B-V$	C_{U-B}		
	V	III	I
−0.30	+1.25		
20	65		+1.48
10	95		60
0.00	2.11		70
+0.10	20		83
20	25		94
30	28		2.05
40	29		16
50	33		28
60	40		39
70	53		50
80	66	+2.72	61
90	80	92	72
1.00	90	3.10	85
10	3.03	28	95
20	15	44	3.06
30	27	57	18
40	40	70	28
50	51	81	38
60	63	93	48
70			58

Now we are going to try an explanation of Fig. 5. It is well known that the Balmer jump is greater in the supergiant than in the dwarf so far as the spectral range from later A to F is concerned (**11**). A wavelength region covering the Balmer jump is included in Johnson's $U-B$, but not or less in the corresponding colors on the systems of refractor type. This is because the supergiant's branch in Johnson's diagram crosses the main sequence downwards at about A7, whereas that in our diagram, in Cape's as well as in Arp's does not intersect with the main sequence. Such a circumstance may suggest that the photometric system of refractor type has, as Arp (**6**) already pointed out, a certain advantage over the standard one in separating the luminosity class I from the class V in the spectral region not later than G.

As to the separation between luminosity classes III and V, it is explained quantitatively by considering the monochromatic difference of brightness between

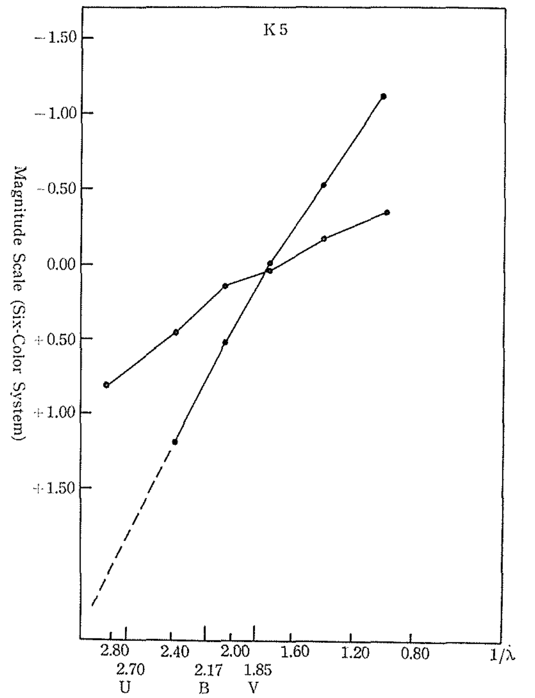

Fig. 13. Whitford's six-color data. *U, B, V* denoted here are in our system.

the normal giant and the dwarf in a similar way to Becker's (**9**) basing on Stebbins-Whitford's six-color photometric data (**12**). Namely, after plotting six colors with regard to both giants and dwarfs for successive spectral types, as illustrated in Fig. 13 with an example for K 5, were read the *U*–, *B*– and *V*–values corresponding to the respective effective wavelengths on our system. We got following values for K5,

	d	*g*	*g–d*
U	+0.72	+1.82	
B	+0.26	+0.78	
V	+0.07	+0.17	
U–B	+0.46	+1.04	+0.58
B–V	+0.19	+0.61	+0.42

Then, the differences of two-color indices between the giants and the dwarfs were found, which are not anything but the giant's location relative to the dwarf's in the two-color diagram. The giant's location computed in this way is represented by a dotted line in Fig. 5. It is said that coincidence with the observations is quite satisfactory.

The same method was applied also to the later supergiants of a few spectral types for which six-color photometric data were available and we found that the calculated supergiant's location shown by a dashed line in the same figure was also in accordance with the observations corrected for space reddening in the way mentioned before. This fact may not only serve as a verification of Arp's intrinsic color for the luminosity class I but open a way for evaluating the space reddening of supergiants. There are two exceptional supergiants of K-type and of M-type which are not on the computed location but far above it. These are both regarded as unreddened in Johnson's list (**4**), but if they were assumed to be reddened, the amount of reddening would be able to obtain from our reddening line. However, the accuracy of our *U*-measure is especially low for the later supergiants, hence the definite conclusion will be left in future.

We do not dare to insist that the two-dimensional spectral classification of stars is capable with sufficient accuracy by only three-color photometry, nevertheless we suggest that even with *U*, *B*, *V* photometry a fair degree of informations on the two-dimensional classification may be accessible by appropriate selection of filters, and yet also, the estimation of space reddening of supergiants may not be impossible.

Acknowledgements

The authors are indebted to Mr. Y. Nakai for designing the first D. C. amplifier and the photometer head, and to Mr. Y. Niimi for help in the observations respectively. They also wish to thank Messrs Y. Shimazu and K. Osawa of Nippon Denkikizai Co., Ltd. for the construction and adjustment of the amplifier.

This investigation has been carried out by a research-grant from the Ministry of Education.

REFERENCES

1. H. L. JOHNSON and W. W. MORGAN, Ap. J. **117** (1953), 313 and Ap. J. **114** (1951), 522.
2. G. E. KRON, Ap. J. **115** (1952), 1.
3. H. L. JOHNSON and D. L. HARRIS, Ap. J. **120** (1954), 196.
4. H. L. JOHNSON and W. W. MORGAN, Ap. J. **117** (1953), 313.
5. H. L. JOHNSON, Ann. d'Ap. **18** (1955), 292.
6. H. C. ARP, A. J. **63** (1958), 118.
7. Cape Mimeogram No. 5 (1958).
8. W. G. TIFFT, A. J. **63** (1958), 127.
9. W. BECKER und U. STEINLIN, Zs. f. Ap. **39** (1956), 188.
10. H. C. ARP, *Handbuch der Physik* Vol. 51 (1958), p. 83.
11. For example, A. UNSÖLD, *Physik der Sternatmosphären* (1954), p. 59.
12. J. STEBBINS and A. E. WHITFORD, Ap. J. **102** (1945), 318;
J. STEBBINS and G. E. KRON, Ap. J. **123** (1956), 440.

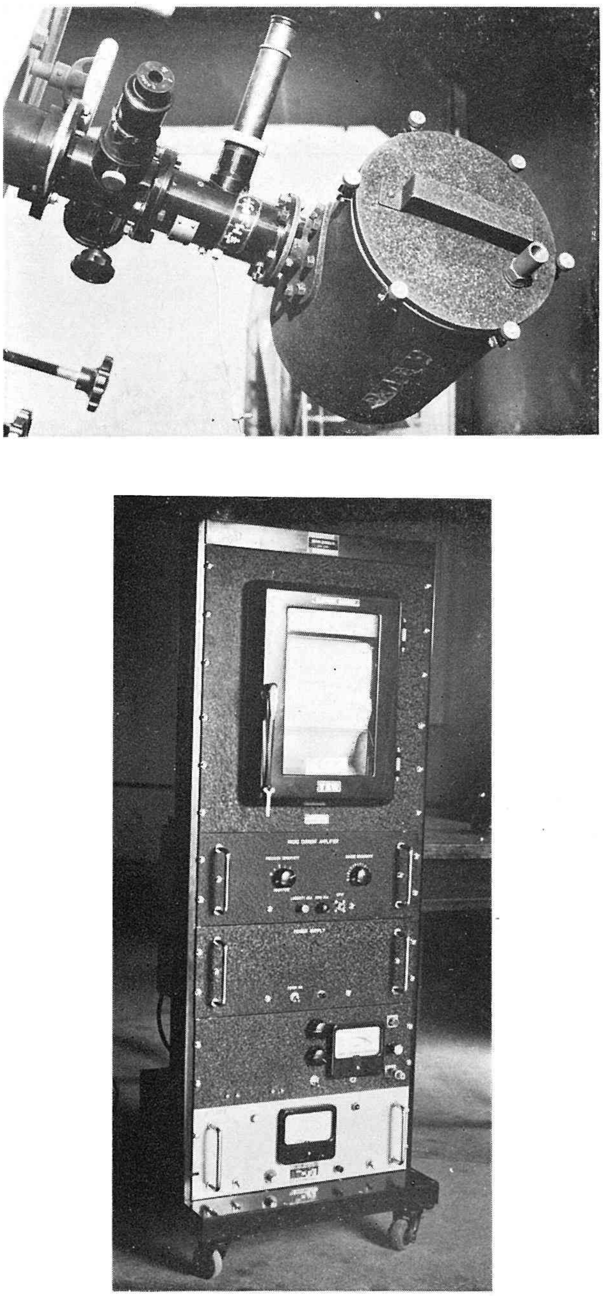

General view of the photometer head, the amplifier and the recorder